Elsevier Editorial System(tm) for Microporous & Mesoporous Materials
Manuscript Draft

Manuscript Number: MICMAT-D-14-00550R1

Title: Liquid droplet evaporation from buckypaper: on the fundamental properties of the evaporation profile

Article Type: SI: Characterization of Porous Solids X

Keywords: evaporation profile; carbon nanotube; buckypaper; drying; sensor

Corresponding Author: Dr. Akos Kukovecz, PhD

Corresponding Author's Institution: University of Szeged

First Author: Gábor Schuszter

Order of Authors: Gábor Schuszter; Erzsébet-Sára Bogya; Dezső Horváth; Ágota Tóth; Henrik Haspel; Akos Kukovecz, PhD

Manuscript Region of Origin: HUNGARY

Abstract: Buckypaper is a mesoporous, self-supporting, electrically conducting mat of multiwall carbon nanotubes prepared by filtering a nanotube suspension through a submicron pore diameter membrane and drying the filter cake. Multiple phenomena take place simultaneously when a liquid droplet contacts the buckypaper surface: wetting, spreading, adsorption, capillary filling, evaporation from the surface, evaporation from the pores, infiltration of nanotube-nanotube junctions, gravity induced convective flow, etc. The electrical resistance of the buckypaper as a function of time exhibits a maximum curve during these processes. The fine details of the shape of this curve are slightly different for every solvent. We refer to this characteristic function as the evaporation profile of the studied liquid. In this paper we combine simultaneous electrical resistivity measurement, weight measurement and visible image processing methods to reveal the basic properties of the evaporation profile. A good correlation between the changes in buckypaper mass and electrical resistance was found and the distribution of the liquid penetrating the buckypaper matrix followed specific patterns and was correlated with the shape of the measured evaporation profile. Results are compared with fluid dynamic simulations. The evaporation profile emerges as a reproducible and inexpensive qualitative analytical tool for liquid identification. Alternatively, recording the evaporation profile of a chosen test liquid could become a feasible characterization method for mesoporous materials.

Response to the comments of the Reviewers

Dear Professor Philip Llewellyin,

Thank you for your decision letter based on the reviewers' comments for our manuscript "Liquid droplet evaporation from buckypaper: on the fundamental properties of the evaporation profile" manuscript. We greatly appreciate the constructive comments.

On the following pages, we outline point-by-point our responses to the comments by the reviewers. We believe to have answered every issue in sufficient detail, but of course we would be glad to respond to any further questions and comments that you may have.

We look forward to hearing from you regarding our submission.

Best regards,

Ákos Kukovecz

Ms. Ref. No.: MICMAT-D-14-00550

Title: Liquid droplet evaporation from buckypaper: on the fundamental properties of the evaporation profile

Microporous & Mesoporous Materials - Reviewers' comments:

Reviewer #1: *The authors have prepared buckypapers with different pore sizes and have studied the evaporation process of different pure liquids. They present a simple model for describing the behavior of the time evolution of the mass of liquid remaining in the liquid, from which the electrical resistence of the buckypaper can be obtained. The experimental and calculated values are in reasonable agreement. There are several questions that the authors have to clarify before the manuscript can be accepted.*

1.- What is all the work useful for? The authors do not mention any application for which the present results improve the existing methods. They mention that since each liquid presents different evaporation profiles, they can be used to identify liquids. First, there are many analytical methods that are very precise and are able to detect and identifie very small samples. Second, the authors present the results for three liquids that have very different chemical nature, is the method able to distinguish between isomers? The second application that the authors mention is the characterization of the mesoporous structure.

However, the method is not suitable for obtaining the pore-size distribution, while other techniques available give that information. Moreover, there are limitations such as those mentioned in the results (section 3.2), so that depending on the nature of the liquid and the thickness and size pore the simple cannot be measured. Other techniques do not have such a shortcomings. The method is limited to conducting mesoporous samples.

We agree with the Reviewer that in its present version, evaporation profile measurement is not such a mature analytical method like chromatography or adsorption-based pore size determination techniques. Indeed, the main reason for doing this work is to learn more about the very complex interface phenomena related to liquid evaporation from a nanoporous matrix. This is why we emphasize already in the title that the manuscript is about the *fundamental* properties of the evaporation profile, not a direct demonstration of its analytical capabilities on a scale that would compete with commercial methods. We find the chance to develop a new method intellectually challenging and believe that science can be advanced through such fundamental studies as well as by more applied research.

Nevertheless, it may actually become possible to find a market for the evaporation profile measurement method in analytical chemistry due to its extreme simplicity. Although in the present method we used simultaneous resistance measurement, imaging and weight measurement to get the complete picture, the evaporation profile itself is actually just the electrical resistance vs. time function, which could be measured by even the simplest instrumentation. Other liquid identification techniques working with microliter-size droplets usually require either some sort of flow control and detector (GC, TLC, ion trap MS) or at least a light source and some optical elements (spectroscopy, index of refraction measurement etc.). On the other hand, the whole instrument necessary for evaporation profile measurement consists of a few mm^2 conductive porous film and a d.c. meter. We do not find it so difficult to envision specialized field applications where such low cost and small physical size would be favoured over the higher performance of existing analytical methods.

The Reviewer is correct to observe that the tested liquids are very different chemically. This was a deliberate choice from our side, since our intention was to introduce the capabilities and limitations of the method on a target analyte scale as broad as possible. A second study involving 17 different organic solvents has been completed since the submission of this manuscript. We have found that the evaporation profiles of the solvents are sufficiently different to serve as a basis for their identification with over 90% accuracy. This study involved the successful identification of the isomers 1-propanol and 2-propanol based on their differing evaporation profiles. Further studies on more isomers are currently underway and will be reported later.

Concerning the characterization of porous materials with the evaporation profile method, we agree with the Reviewer that there are other methods with better performance available. On the other hand, it is obvious that the fine structure of the evaporation profile is influenced by the porosity and wall surface properties of the film; therefore, we see no fundamental reason why the method could not be developed into a specialized characterization method in the future. Nevertheless, the corresponding sections of the abstract and the manuscript text were rephrased so that the strength of the statement about the applicability of the method for porous material characterization is reduced a bit.

2.- *Some years ago Starov and Velarde studied the spreading over porous substrates and they obtained a universal curve. This paper should be included in the Reference list.*

Thank you for drawing our attention to this paper. In the introduction part at page 4 the study by Starov and Veladre on the spreading and wetting of micrometer sized porous thin layers is now cited.

3.- *Section 2.2: The precisión of the balance should be given because the size of the drops is very small.*

The precision of the Oertling - WA205 micro balance is 4 point decimal (0.1 mg). This information has been added to the text.

4.- *Last paragraph of page 7: The authors indicate that the results are not reproducible unless the same buckypaper is used. They have to explain why. Is this because each buckypaper simple is different? Otherwise the method proposed is quite useless.*

Thank you for drawing our attention to this ill-phrased statement. Actually, the situation is this:

- The evaporation profile of any liquid that we tested can be measured very reproducibly on the same buckypaper.
- The shape descriptor parameters of the evaporation profile (e.g. time to reach maximum peak height, decay time from peak maximum to 50%, 25% and 10% intensity etc.) are very reproducible even between different buckypaper samples.
- Our original statement referred to the absolute peak height, which does indeed vary by approx. 20% from buckypaper to buckypaper, because each sample has a slightly different structure. However, since real analytical information is always derived from the shape descriptor parameter vector and not the absolute peak height itself, this variation does not affect the usability of the method adversely at all.

The text in the manuscript has been rephrased to mirror this information.

5.- Last line of page 9 and first line of page 10: The sentence "We refer to this function....." has already be written previously.

Thank you for noticing this! The sentence "We refer to this function....." was deleted from page 10 and the previous sentence was modified : "…the electrical resistance of the film exhibits a very characteristic change as a function of time, the evaporation profile."

6.- Reference 1: The title should not be in capital characters.

Corrected, thank you!

7.- *Figure 1: I recommend to give a more detailed description of the set-up in the text (experimental section). There are aspects that are not completely clear, e.g. how the electrical contacts are made, to which extend the rigidity of the electrical wires affect the response of the balance. More intriguing is how the spreading and complete embebding of the samples take place is less than 2 seconds,*

where measurements of the EP start to be taken. Which tests have the authors performed for checking this?

Thank you for drawing our attention to this issue. Section 2.2 of the manuscript has been amended based on this comment. Electrical contacts to the film were made by copper film on the plastic sheet (which was actually a PCB board). The copper electrodes were contacted to the source meter by 0.3 mm diameter copper wires. The rigidity of these wires did not affect the balance at all because of the large inertia of the whole assembly mounted on the balance plate. This was confirmed by independent experiments before the evaporation profile measurements.

When measuring the evaporation profile, the buckypaper was mounted in the assembly and heating was applied until the electrical resistance and the sample weight both stabilized. Then all three recordings (resistivity, imaging and sample weight) were started a few seconds before dropping the analyte droplet onto the film. Therefore, all measurements were running already when the spreading and embedding of the liquid droplet commenced. All elements of the system were tested dry before any EP measurements to exclude any artefacts introduced by the measurement itself.

Reviewer #2: *The paper by Schuszte et al., argues the use of droplet evaporation as a method for surface characterization. Here MWCNT films were used with 1-propanol as wetting fluid and the electrical resistance of the system followed. Acetone and DMF were further used as solvents. The publication can accepted as is, with one minor error with an unknown symbol on page 7, at 10 lines from bottom (maybe µ).*

Corrected, thank you!

*Highlights (for review)

Liquid droplet evaporation from buckypaper: on the fundamental properties of the evaporation profile

Highlighs:

- the evaporation of a liquid drop from a mesoporous carbon nanotube mat is studied
- “evaporation profile” is defined as the R vs. t function of a drying material
- correlations between the mass, resistance and pore filling are revealed
- evaporation profile measurement emerges as a new analytical method

*Graphical Abstract (for review)

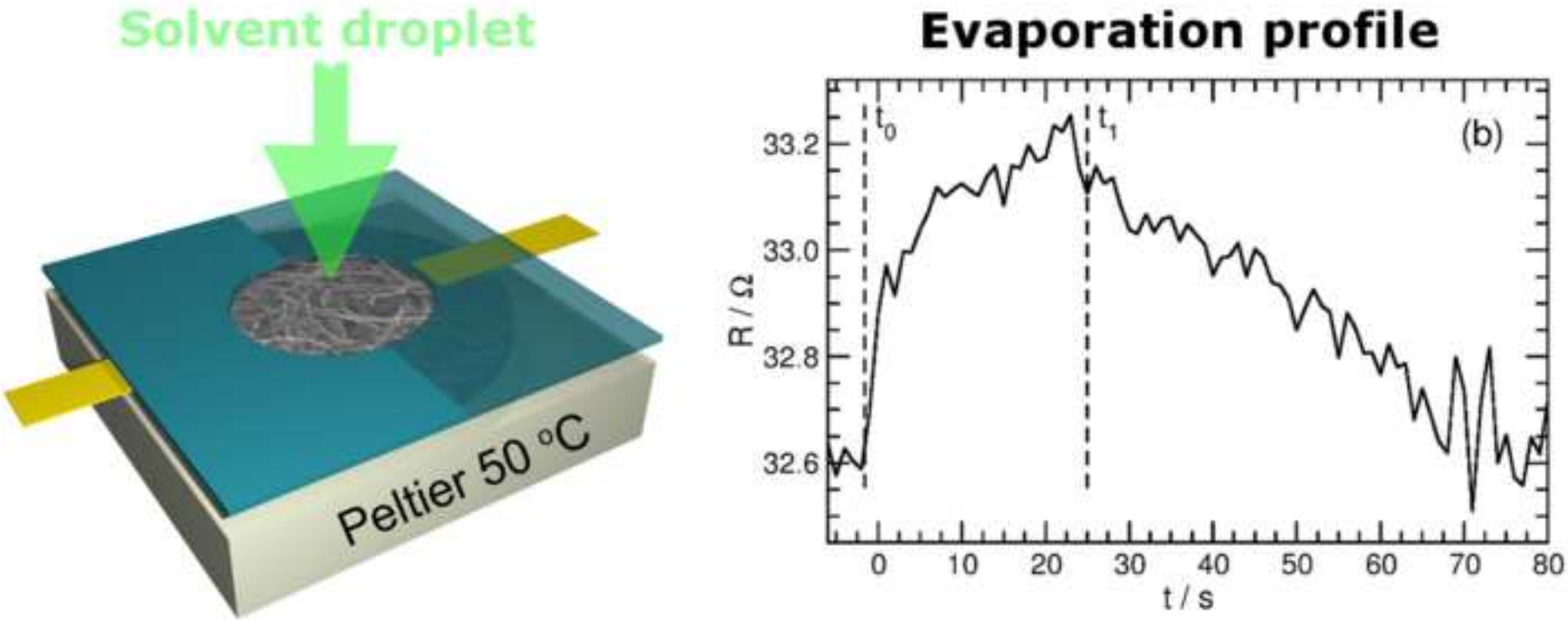

Liquid droplet evaporation from buckypaper: on the fundamental properties of the evaporation profile

Gábor Schuszter[1], Erzsébet-Sára Bogya[2], Dezső Horváth[1], Ágota Tóth[1], Henrik Haspel[3], Ákos Kukovecz[2,3,*]

[1]Department of Physical Chemistry and Materials Science, University of Szeged, Rerrich Béla tér 1, Szeged, H-6720, Hungary

[2]MTA-SZTE "Lendület" Porous Nanocomposites Research Group, Rerrich Béla tér 1, Szeged, H-6720, Hungary

[3]Department of Applied and Environmental Chemistry, Rerrich Béla tér 1, Szeged, H-6720, Hungary

***Corresponding author:**

Ákos Kukovecz, Ph.D.

Department of Applied and Environmental Chemistry

University of Szeged

H-6720 Szeged, Rerrich Béla tér 1.

Hungary

Email: kakos@chem.u-szeged.hu

Phone: +36-62-544-620

Fax: +36-62-544-619

Abstract

Buckypaper is a mesoporous, self-supporting, electrically conducting mat of multiwall carbon nanotubes prepared by filtering a nanotube suspension through a submicron pore diameter membrane and drying the filter cake. Multiple phenomena take place simultaneously when a liquid droplet contacts the buckypaper surface: wetting, spreading, adsorption, capillary filling, evaporation from the surface, evaporation from the pores, infiltration of nanotube-nanotube junctions, gravity induced convective flow, etc. The electrical resistance of the buckypaper as a function of time exhibits a maximum curve during these processes. The fine details of the shape of this curve are slightly different for every solvent. We refer to this characteristic function as the evaporation profile of the studied liquid. In this paper we combine simultaneous electrical resistivity measurement, weight measurement and visible image processing methods to reveal the basic properties of the evaporation profile. A good correlation between the changes in buckypaper mass and electrical resistance was found and the distribution of the liquid penetrating the buckypaper matrix followed specific patterns and was correlated with the shape of the measured evaporation profile. Results are compared with fluid dynamic simulations. The evaporation profile emerges as a reproducible and inexpensive qualitative analytical tool for liquid identification. Alternatively, recording the evaporation profile of a chosen test liquid could become a feasible characterization method for mesoporous materials.

Keywords: evaporation profile; carbon nanotube; buckypaper; drying; sensor.

1. Introduction

Even though carbon nanotubes are known for over 20 years [1], the international scientific community is as interested in them as ever [2]. However, the majority of research efforts focused on carbon nanotubes (CNTs) is dealing either with individual nanotubes (e.g. transistors, sensors) or with large assemblies of tubes (e.g. catalyst supports) [3]. Self-supporting porous multiwall carbon nanotube films (MWCNT paper or buckypaper) prepared by the filtration of a nanotube suspension are found in between these two extremes. Although buckypaper has been used for a long time to ease the handling of macroscopic amounts of carbon nanotubes, it was only recently that research on the interesting properties owing to the porous buckypaper form itself was initiated.

Buckypaper is a layered mesoporous material with a typical pore diameter of 25-40 nm which can be tuned by changing the length of the filtered nanotubes [4]. The Young modulus of buckypaper is 0.6–4.2 GPa and its tensile strength is 6–33 MPa [5],[6],[7]. CNT films are good conductors of heat and electricity. Unoriented MWCNT films exhibit a thermal transport coefficient of 15 $W \cdot mK^{-1}$ [8], however, by magnetic alignment it was possible to increase this value up to 42 $W \cdot mK^{-1}$ [9]. Carbon nanotube films have several interesting applications radiofreqency filters [10], artificial muscles [11], cold field emission cathodes [12], mechanical sensors [13], semiconducting layers in different types of electronic, optoelectronic, and sensor systems [14] or as starting materials for SiC nanorod synthesis [15].

The evaporation of a drop from the surface/pores of porous materials is a complex process, combining several consecutive and parallel steps, like: drop impact on the surface, spreading and wetting, solvent diffusion into pores, evaporation from the surface and pores, etc. Although certain steps of this process have been already

studied and models were developed to explain the effect of surface/solvent characteristics on the process development, there are many unanswered questions left to debate. Each step is complex by itself, and to our best knowledge, the whole problem has not yet been treated as a continuous process in any model.

The behaviour of a drop upon impact on a porous material depends on droplet diameter, impact speed, impact angle, viscosity, surface tension, temperature, material properties, etc. [16]. Wetting in general is a phenomenon that spans over two length scales, macroscopic (hydrodynamics) and microscopic (molecular). The spreading/wetting of a solvent on a surface is due to the interaction of a liquid with a solid, and the mechanisms governing the wetting behaviour are still not completely understood [17]. Spreading and wetting of micrometer sized porous membranes by liquid droplets was studied by V.M. Starov et al. [18-20]. The spreading of liquid drops over thick porous layers was discussed for two cases complete and partial wetting, the process being divided in two, respectively three stages. Over the duration of the first stage the imbibition front inside the porous layer expands slightly ahead of the spreading drop and in the second final stage the drop base starts to shrink until the drop completely disappears and the imbibition front expands until the end of the process. Although the spreading and wetting topic is meticulosity presented, the problematic of evaporation from the pores is not discussed. Also the wetting at nanometer scale raises the necessity to investigate the flow of liquids inside nanochannels, as channel wettability plays an integral role in the flow of liquids through it [21]. A coherent theoretical framework relating wettability to fluid flow in nanochannels is still missing despite a large number of experimental papers having been published [22].

The capillarity of nanotubes is directly related to the surface energies of interaction between the liquid and the solid surface. The Young-Laplace equation connects the pressure difference (ΔP) to the surface tension of the liquid (γ) and the contact angle between the solid and the liquid (θ):

$$\Delta P = 2\gamma \cos\theta r^{-1} \qquad (1)$$

where r is the radius of the curvature of the meniscus. If θ is smaller than 90° then the liquid will be spontaneously pulled into a capillary as there is an energy gain in the process [16].

Evaporation from porous media is of great interest to numerous industrial applications including the drying of agricultural and pharmaceutical products, light oil recovery, soil remediation, construction [23], drop or spray deposition in industrial, agricultural and biomedical environments and the cooling of metallic and ceramic surfaces and of electronic devices [21]. Several experimental studies [24, 25] and theoretical models [24, 25], [26] were developed to understand solvent evaporation from three-dimensional pore networks. Liquid wetting and evaporation were monitored by different experimental methods: environmental scanning electron microscopy [27], highly-resolved neutron radiography [28], transmission electron microscopy [29], contact angle measurements [17],[30] and high speed camera recordings[31], [32]. Mostly the contact angle, base area, drop volume/radius/weight evolution in time were monitored. However, despite much research and process modeling during the last 20 years, droplet evaporation from porous surfaces remains only partially understood.

In this paper we present a new approach on solvent evaporation monitoring from porous materials. When a solvent is dropped onto the surface of a CNT film, the resistance/time function shows a characteristic curve with one maximum. The fine

details of the shape of this curve (time to reach the maximum, full width at half maximum, shape of the tail etc.) are slightly different for every solvent. That is why a new terminology is introduced to describe the solvent droplet – porous material interaction. The electrical resistance (R) as a function of time (t) is termed as the "evaporation profile" (EP) of the solvent. The goal of this work is to determine the basic characteristics (EP fine structure determination, drop radius variation in function time, wetting section shape and depth definition, etc.) of droplet evaporation from buckypaper. Moreover, we will explore if the evaporation profiles of different liquids can be distinguished from each other. Our ultimate goal is to establish evaporation profile measurements as a rapid and inexpensive qualitative solvent analysis tool as well as a mesoporous material characterization method.

2. Experimental

2.1 Carbon nanotube film preparation

The MWCNTs were synthesized in our laboratory using the catalytic chemical vapor deposition (CCVD) process described earlier [33]. This reaction is known to yield closed MWCNTs over 10 μm in length with outer and inner diameters of 15–25 nm and 3–6 nm, respectively. Our standard nanotube purification protocol involves oxidative and acid leaching steps, therefore, the surface of the synthesized nanotubes contains –OH and –COOH functional groups and is consequently moderately hydrophilic. Although not used in this work, it is worth noting that the hydrophilic/hydrophobic surface balance can be precisely tuned by the high temperature annealing of the nanotubes if necessary [34].

Carbon nanotube films (buckypapers) were prepared from calculated amounts (3, 5 and 10 mg) of MWCNTs suspended in 50 cm^3 dimethyl-formamide (DMF)

solvent by 30 min sonication in an ultrasonic bath [35]. The suspensions were filtered through 0.45 μm Whatman nylon filters using dead-end filtration with an effective pressure difference of 960 mbar. The samples were dried at 70 °C overnight in air on the filters and peeled off afterwards. Methods to control the average pore diameter [36], the pyroelectric response [4] and the gas permeability [37] of buckypaper prepared by this method were reported in our earlier communications.

2.2 Evaporation profile recordings

The experimental setup used for recording the evaporation profile is shown in Fig. 1. A plastic plate with a 0.6 cm radius gap in the center was equipped with two copper electrical connections at the opposite edges of the gap on the bottom of the sheet. The buckypaper was fixed to the bottom of the plastic section with dielectric clips. The assembly was placed on an analytical balance (Oertling - WA205, 0.1 mg precision) linked to a data acquisition computer. The computer simultaneously recorded the electrical resistance of the buckypaper as measured by a Keithley 2612A Source Meter and collected top-view images provided by a monochrome charge-coupled device camera (Unibrain -The 1394 Innovators) at 1 frame per second rate. A Peltier cell under the plastic plate served as a heating source. The distance between the CNT plate and the heater was set to 1 cm, so the temperature was constant (50 °C) throughout the experiment. The temperature stability was checked in an independent measurement and was found to be better than 0.1 °C.

The copper electrodes were contacted to the source meter by 0.3 mm diameter copper wires. The rigidity of these wires did not affect the balance because of the large inertia of the whole assembly mounted on the balance plate. This was confirmed

by independent experiments before the evaporation profile measurements. When measuring the EP, the buckypaper was mounted in the assembly and heating was applied until the electrical resistance and the sample weight both stabilized. Then all three recordings (resistivity, imaging and sample weight) were started a few seconds before dropping the analyte droplet onto the film.

The basic shape and characteristics of the evaporation profile were determined by dropping 3 μl of 1-propanol on the buckypaper surface and the electrical resistance variation as a function of time was monitored. The effect solvent type and volume on the EP were studied by dropping a single droplet (3 or 5 μl) of a solvent (acetone, 1-propanol or N,N-dimethyl-formamide) to the center of the CNT film and simultaneously recording the mass and electrical resistance until they returned to their original values (baseline). Images taken at various stages of liquid evaporation were analysed by our own evaluation software. The evaporation profiles of the same analyte on the same buckypaper were found to be very reproducible. Moreover, the shape descriptor parameters (e.g. time to reach maximum height, decay time from maximum to 50%, 25% and 10% intensity) matched very well when repeating the EP measurement with the same analyte on different buckypapers. The absolute peak height of the EP exhibited approx. 20% variation from buckypaper to buckypaper because of the experimental variations in the microstructure of each MWCNT film.

XXX insert Figure 1. here please XXX

3. Results

The detailed morphological and N_2 adsorption analysis of the buckypapers was published earlier [38]. The nanotubes in the buckypaper measure 15-25 nm in

diameter and several tens μm in length and are not bundled [36]. Their dominant orientation is normal to the direction of the filtration. The film has a layered structure, which is attributed to the filtration. The thickness of an individual layer is approx. 1 μm, the whole buckypaper is 140 μm thick and its apparent pore diameter (formed by intertube spaces) follows a lognormal distribution with d=39 nm, σ=12 nm.

3.1 1-propanol droplet evaporation

When dropping 1-propanol on the CNT film, the liquid starts to diffuse immediately into the pores of the buckypaper, but a part of it remains spread on the surface of the film (see Fig. 2a). The evaporation of this liquid from the surface takes place together with the diffusion. Once all 1-propanol evaporates from the surface, liquid is left only in the pores. The whiter spot from Fig. 2b represents the area where the solvent diffused into the buckypaper. The solvent gradually evaporates from the pores as well because of the continuous heating. The solvent free image of the film is captured in Fig. 2c. The complete evaporation of the solvent was confirmed by the fact that the electrical resistance of the buckypaper returned to the baseline.

XXX Insert Figure 2. here please XXX

The electrical resistance and mass of the buckypaper increased as soon as the solvent was dropped to the film. The resistance and mass variation are illustrated in Fig. 3. where t_0 marks the time when the drop was instilled. The time needed to surface evaporation is marked with t_1. The abrupt weight increase to the maximum in Figure 3a. is due to the landing of the 1-propanol droplet on the buckypaper surface at t_0. This is followed by a quasi-linear weight decrease till t_1. It should be noted that the

electrical resistance increases continuously t_0 between and t_1, because in this interval the solvent fills the pores of the MWCNT film and the resistance of the solvent occupied section is higher than the liquid-free one.

XXX Insert Figure 3. here please XXX

Once the primary surface evaporation is complete (t_1), both the electrical resistance and the mass of the buckypaper decrease as linear (within experimental error) functions of time due to the continuous evaporation of the solvent. Evaporation takes place both within the buckypaper pores (resulting in 1-propanol vapor diffusing to the atmosphere) and from the surface where capillary forces continue to deliver liquid from the inside of the buckypaper (secondary surface evaporation). Fig. 4. Demonstrates that there is a linear correlation between the remaining 1-propanol weight and the electrical resistance of the buckypaper. Both the mass and the electrical resistance return to their original baseline values by the end of the drying process and neither of these functions is influenced by the initial mass of the buckypaper itself.

XXX Insert Figure 4. here please XXX

Summarizing, when a droplet of solvent contacts a heated mesoporous multiwall carbon nanotube film, the electrical resistance of the film exhibits a very characteristic change as a function of time, the evaporation profile. Although in principle it would also be possible to define the EP as the variation of film weight over time, the time dependence of the electrical resistance exhibits a more complex behaviour (which translates into additional information contents) between t_0 and t_1 and therefore, it is a more suitable basis for an analytical method.

The relationship between the intensity and the radius of the whiter spot (the solvent wetted area of the buckypaper) was investigated during evaporation in the recorded visible camera image series. The spot radius decreased only slowly but the intensity dropped significantly in time as shown in Fig. 5a. Therefore, there must be a correlation between the integrated intensity of the spot and the mass of the liquid remaining in the buckypaper at any given time. Fig. 5b. confirms that a linear relationship indeed exists between the integrated spot intensity and remaining solvent weight at any given time during the drying process.

XXX Insert Figure 5. here please XXX

The mass of the liquid present in the pores at a time can be determined from the spot intensity. The porosity of the CNT plate (ε) was defined as the fraction of the liquid volume (V_f) and the total volume of the CNT sheet (V):

$$\varepsilon = \frac{V_f}{V} \qquad (2)$$

where $V = \bar{h} r^2 \pi$, and $\bar{h}$ is the average thickness of the MWCNT film at the spot where the solvent was dropped and r is the radius of that spot. The mass of the solvent (m) is expressed as a function of liquid volume (V_f) and the its density (ρ):

$$m = \rho V_f = \rho \varepsilon V = \rho \varepsilon \int_0^\infty 2\pi h(r) dr \qquad (3)$$

with

$$h(\mathrm{r}) = \mathrm{k}\left[I(\mathrm{r}) - I_\infty(\mathrm{r}) \right] \qquad (4)$$

where k is a constant, $I(r)$ and $I_\infty(r)$ are the measured spot intensities along the r radius in time and after the disappearance of the spot, respectively. Substitutions yield:

$$m = 2\pi\rho\varepsilon k \int_0^\infty \left[I(\mathrm{r}) - I_\infty(\mathrm{r}) \right] r dr = 2\pi\rho\varepsilon k \left[\int_0^\infty I(\mathrm{r})\,\mathrm{r}\,dr - \int_0^\infty I_\infty(\mathrm{r})\,\mathrm{r}\,dr \right] \quad (5)$$

After rearrangements it is obtained:

$$\int_0^\infty I(\mathrm{r})\,\mathrm{r}\,dr = \frac{1}{2\pi\rho\varepsilon k} m + \int_0^\infty I_\infty(\mathrm{r})\,\mathrm{r}\,dr \quad (6)$$

The plot of the integrated intensity as the function of the solvent mass gives a straight line with a slope of *M* from which the *k* constant from equation 4 can be determined as:

$$k = \frac{1}{2\pi M \rho\varepsilon} \quad (7)$$

The thickness of the liquid-containing CNT film can then be calculated from the graphical representation of *h(r)* as a function of the spot radius at any time. The result is shown in Fig. 6 for a few selected stages of the drying process. The maximum thickness of the wetted section was found to be 65 μm. This appears to be a realistic estimation since the total thickness of the CNT film was 140 μm as determined from an independent measurement.

XXX Insert Figure 6. here please XXX

3.2 Evaporation profiles of other solvents

Having examined the basic evaporation properties of a 1-propanol droplet from the surface and pores of a mesoporous MWCNT film, further experiments were carried out with acetone and N,N-dimetyl-formamide (DMF) in order to elucidate the differences and similarities of the evaporation phenomenon. The same general observations could be made: (i) The solvent first spreads and wets the surface then

diffuses into the pores of the CNT film, but some solvent remained on the surface of the buckypaper; (ii) the drop evaporates relatively fast because of the heating. The evaporation time (10 - 400 s) depends on the solvent type, droplet volume and the mass (linearly correlated with the thickness) of the buckypaper; (iii) after the primary surface evaporation solvent was found in the pores only. In the captured images a whiter spot marks the section where the solvent diffused into the pores.

Figure 7. depicts the buckypaper weight variation as a function of time for the three solvents. Although the volume of the droplet was constant, the maximum of the curves is different because of the differing liquid densities. Weight loss was a linear function of time for all three solvents but the slopes were different for each liquid, therefore, the time required for the mass to return to baseline was also different. As expected (Table 1.) the highest evaporation rate was observed for acetone and the lowest for DMF.

XXX Insert Figure 7. here please XXX

XXX Insert Table 1. here please XXX

The time dependence of the electrical resistance was always similar to the 1-propanol case: resistance increased until the end of the primary surface evaporation step and decreased quasi linearly to baseline again afterwards. This linear decrease phase is illustrated with electrical resistance vs. remaining solvent weight functions in Fig. 8. Lines denote linear fits to the experimental data.

Evaporation profile experiments were carried out with 3, 5 and 10 mg CNT films and with 3 and 5 μl solvent droplets. For acetone only one set of experimental results is presented (5 mg CNT plate mass and 3 μl solvent volume), because in the case of 3 mg film the acetone could drench the whole plate, hence solvent could

evaporate from both sides of the plate. On the other hand, the 10 mg buckypaper proved to be too thick for acetone to give any detectable electrical signal in our experimental setup.

The results of all these EP experiments are summarized in Table 2. which contains the weight of the CNT plate (m), the solvent droplet volume (V), the average slope of the fitted resistance-weight curves, the maximum thickness of the liquid-filled area (h) and the maximum radius of the wetted section (r). The thickness of the liquid-containing CNT plate was calculated with equation 4.

XXX Insert Figure 8. here please XXX

XXX Insert Table 2. here please XXX

Data DMF on 3 mg buckypaper is missing because the solvent has spread to the whole film surface. In other cases the *h* value increases and *r* decreases with increasing buckypaper mass for the same solvent volume. The same pattern can be observed for different solvent volumes at 10 mg films with 1-propanol and DMF. If the film mass (5 mg) and solvent volume (3 μl) were kept constant and the solvents were varied, then differences in the *h* and *r* values were observed. The highest *h* and the smallest *r* values were found for acetone. In the case of 1-propanol the maximum radius of the wetted section was higher and the *h* value was smaller, indicating that less 1-propanol diffused into the pores than other solvents. On the other hand, DMF exhibited the highest spreading affinity, which manifested in a small *h* and high *r* value (Fig. 9.).

XXX Insert Figure 9. here please XXX

4. Discussion

The electrically conductive buckypaper was modeled as a thin slab with two different specific conductivities. In the gas-filled (liquid-free) area of the sheet the specific conductivity (k_g) is set higher than the specific conductivity of the liquid-filled area (k_l). Since current can enter the CNT plate only at one point and can leave it also at a single location only, the zero-flux boundary condition can be applied as illustrated in Figure 10. Ohm's law in differential form was used to calculate the resistance of the whole film:

$$\vec{j} = -\frac{1}{\rho}\nabla U \qquad (8)$$

where $\vec{j}$ is the current density with div $\vec{j}$ =0, while ρ is the specific resistance and U is the potential. The rearrangement of the equation leads to:

$$\nabla \cdot \vec{j} = \kappa \nabla^2 U \qquad (9)$$

where k is the resultant conductivity.

XXX Insert Figure 10. here please XXX

Before solvent dropping the MWCNT mat is liquid-free so in every point $k=k_g$ in Equation 9. The calculations were designed systematically, by changing the value of k_g but limiting the simulation by the factor that the calculated and the measured resistances have appropriate values within their respective established error ranges. After establishing the k_g value, the case when the solvent evaporates only from the film surface was taken into consideration. Than $k=k_g$ for solvent-free sections and $k=k_l$ where the pores are liquid filled. The calculations have also been run systematically by changing the value of k_l, while the calculated and the measured resistances were kept at approximately the same value.

The software OpenFOAM-1.6 was used to model the dispersion of the electrical resistance of the film. A mesh was created to represent the real sheet and

three different resolutions were used for the simulations: 200 x 200 x 7 for 3 mg films, 200 x 200 x 14 for 5 mg and 200 x 200 x 19 for 10 mg buckypaper. These resolutions were set because the thickness of the CNT sheets depends on the weight of the film. After setting the specific conductivity values (k_g,k_l) the calculations were run on every picture frame for the intermediary phase where the solvent droplet had already evaporated from the film surface but the liquid was still present within the pores.

The comparison between the calculated and the measured resistance values is shown in Figure 11. The calculated values agree well with data measured for acetone and 1-propanol. In the case of DMF instillation after total solvent evaporation, a blanch white spot was detected on the surface of the film even though the electrical resistance and the buckypaper weight have returned to their baseline values. This unusual behavior was also noticed during the image evaluation, hence the DMF experiments were not taken into further consideration. This phenomenon is similar to the formation of a stain after the drying of a spilled coffee drop on a surface. This can be caused by nanoparticle dispersion in DMF and structure formation during evaporation, which leaves a mark on the surface of the buckypaper [34].

XXX Insert Figure 11. here please XXX

The calculated specific conductivity dispersion is shown in Figure 12. The red color corresponds to the solvent filled section of the film and the blue area is the liquid-free section after solvent evaporation from the surface. The maximal diameter of the solvent-filled area is about 5 mm and the average film thickness is 60 μm for 5 mg CNT film with 3 μl propanol. Fig. 12b illustrates the buckypaper cross section magnified 10 times in order to illustrate the image-based estimated shape of the solvent filled area.

XXX Insert Figure 12. here please XXX

5. Conclusions

The time dependence of the electrical resistance of mesoporous multiwall carbon nanotube films upon dropping a small amount of organic solvent on their surface was studied. The resulting R vs t functions were termed as evaporation profiles. A very good linear correlation between the changes in the weight and the electrical resistance of the drying nanotube membrane was found. We also noticed that the distribution of the liquid penetrating the buckypaper matrix follows very specific patterns and is directly correlated with the shape of the measured evaporation profile. The EP measurement was coupled with low framerate visible image analysis. From light intensity variation the thickness of the wetted section was approximated and a model was created to describe the evaporation of the solvent from the buckypaper. Experimental and modeled pore filling values agreed well.

Evaporation profiles were found to be reproducible and characteristic for the dropped solvent when comparing the behavior of 1-propanol, acetone and N,N-dimethyl-formamide. We suggest that the evaporation profile can be developed into a rapid and inexpensive tool for qualitative solvent analysis. It seems possible that by fixing the liquid type and varying the mesoporous matrix, the evaporation profile measurement method could be utilized for porous solids characterization as well.

Acknowledgments

The financial support of the Hungarian National Research Fund projects OTKA NN 110676 and K 112531 is acknowledged.

References

[1] S. Iijima, Helical microtubules of graphitic carbon, Nature, 354 (1991) 56-58.

[2] U.N. Maiti, W.J. Lee, J.M. Lee, Y. Oh, J.Y. Kim, J.E. Kim, J. Shim, T.H. Han, S.O. Kim, 25th Anniversary Article: Chemically Modified/Doped Carbon Nanotubes & Graphene for Optimized Nanostructures & Nanodevices, Advanced Materials, 26 (2014) 40-67.

[3] N. Halonen, A. Rautio, A.-R. Leino, T. Kyllonen, G. Toth, J. Lappalainen, K. Kordas, M. Huuhtanen, R.L. Keiski, A. Sapi, M. Szabo, A. Kukovecz, Z. Konya, I. Kiricsi, P.M. Ajayan, R. Vajtai, Three-Dimensional Carbon Nanotube Scaffolds as Particulate Filters and Catalyst Support Membranes, Acs Nano, 4 (2010) 2003-2008.

[4] Á. Kukovecz, R. Smajda, Z. Kónya, I. Kiricsi, Controlling the pore diameter distribution of multi-wall carbon nanotube buckypapers, Carbon, 45 (2007) 1696-1698.

[5] R.H. Baughman, Carbon Nanotube Actuators, Science, 284 (1999) 1340-1344.

[6] J.N. Coleman, W.J. Blau, A.B. Dalton, E. Munoz, S. Collins, B.G. Kim, J. Razal, M. Selvidge, G. Vieiro, R.H. Baughman, Improving the mechanical properties of single-walled carbon nanotube sheets by intercalation of polymeric adhesives, Appl. Phys. Lett., 82 (2003) 1682-1684.

[7] X. Zhang, T.V. Sreekumar, T. Liu, S. Kumar, Properties and Structure of Nitric Acid Oxidized Single Wall Carbon Nanotube Films, The Journal of Physical Chemistry B, 108 (2004) 16435-16440.

[8] D.J. Yang, Q. Zhang, G. Chen, S.F. Yoon, J. Ahn, S.G. Wang, Q. Zhou, Q. Wang, J.Q. Li, Thermal conductivity of multiwalled carbon nanotubes, Physical Review B, 66 (2002) 165440.

[9] P. Gonnet, Z. Liang, E.S. Choi, R.S. Kadambala, C. Zhang, J.S. Brooks, B. Wang, L. Kramer, Thermal conductivity of magnetically aligned carbon nanotube buckypapers and nanocomposites, Current Applied Physics, 6 (2006) 119-122.

[10] N.A. Prokudina, E.R. Shishchenko, O.-S. Joo, K.-H. Hyung, S.-H. Han, A carbon nanotube film as a radio frequency filter, Carbon, 43 (2005) 1815-1819.

[11] U. Vohrer, I. Kolaric, M.H. Haque, S. Roth, U. Detlaff-Weglikowska, Carbon nanotube sheets for the use as artificial muscles, Carbon, 42 (2004) 1159-1164.

[12] W. Knapp, D. Schleussner, Field-emission characteristics of carbon buckypaper, Journal of Vacuum Science & Technology B: Microelectronics and Nanometer Structures, 21 (2003) 557-561.

[13] D. Prasad, L. Zhiling, N. Satish, E.V. Barrera, Nanotube film based on single-wall carbon nanotubes for strain sensing, Nanotechnology, 15 (2004) 379.

[14] Q. Wang, H. Moriyama, Carbon Nanotube-Based Thin Films: Synthesis and Properties, 2011.

[15] E. Muñoz, A.B. Dalton, S. Collins, A.A. Zakhidov, R.H. Baughman, W.L. Zhou, J. He, C.J. O'Connor, B. McCarthy, W.J. Blau, Synthesis of SiC nanorods from sheets of single-walled carbon nanotubes, Chem. Phys. Lett., 359 (2002) 397-402.

[16] T.W. Ebbesen, Wetting, filling and decorating carbon nanotubes, J. Phys. Chem. Solids, 57 (1996) 951-955.

[17] K. Sefiane, M.E.R. Shanahan, M. Antoni, Wetting and phase change: Opportunities and challenges, Current Opinion in Colloid & Interface Science, 16 (2011) 317-325.

[18] V.M. Starov, S.R. Kostvintsev, V.D. Sobolev, M.G. Velarde, S.A. Zhdanov, Spreading of Liquid Drops over Dry Porous Layers: Complete Wetting Case, J. Colloid Interface Sci., 252 (2002) 397-408.
[19] V.M. Starov, S.A. Zhdanov, S.R. Kosvintsev, V.D. Sobolev, M.G. Velarde, Spreading of liquid drops over porous substrates, Adv. Colloid Interface Sci., 104 (2003) 123-158.
[20] V.M. Starov, S.R. Kosvintsev, V.D. Sobolev, M.G. Velarde, S.A. Zhdanov, Spreading of Liquid Drops over Saturated Porous Layers, J. Colloid Interface Sci., 246 (2002) 372-379.
[21] M. Guilizzoni, G. Sotgia, Experimental analysis on the shape and evaporation of water drops on high effusivity, microfinned surfaces, Experimental Thermal and Fluid Science, 34 (2010) 93-103.
[22] S. Bekou, D. Mattia, Wetting of nanotubes, Current Opinion in Colloid & Interface Science, 16 (2011) 259-265.
[23] M. Abuku, H. Janssen, J. Poesen, S. Roels, Impact, absorption and evaporation of raindrops on building facades, Building and Environment, 44 (2009) 113-124.
[24] S.K. Singh, S. Khandekar, D. Pratap, S.A. Ramakrishna, Wetting dynamics and evaporation of sessile droplets on nano-porous alumina surfaces, Colloids and Surfaces a-Physicochemical and Engineering Aspects, 432 (2013) 71-81.
[25] K. Sefiane, L. Tadrist, M. Douglas, Experimental study of evaporating water–ethanol mixture sessile drop: influence of concentration, International Journal of Heat and Mass Transfer, 46 (2003) 4527-4534.
[26] O. Chapuis, M. Prat, M. Quintard, E. Chane-Kane, O. Guillot, N. Mayer, Two-phase flow and evaporation in model fibrous media, J. Power Sources, 178 (2008) 258-268.
[27] R. Wu, G.-M. Cui, R. Chen, Pore network study of slow evaporation in hydrophobic porous media, International Journal of Heat and Mass Transfer, 68 (2014) 310-323.
[28] D. Mattia, V. Starov, S. Semenov, Thickness, stability and contact angle of liquid films on and inside nanofibres, nanotubes and nanochannels, J. Colloid Interface Sci., 384 (2012) 149-156.
[29] N. Shokri, M. Sahimi, D. Or, Morphology, propagation dynamics and scaling characteristics of drying fronts in porous media, Geophysical Research Letters, 39 (2012) L09401.
[30] K. Sefiane, R. Bennacer, Nanofluids droplets evaporation kinetics and wetting dynamics on rough heated substrates, Adv. Colloid Interface Sci., 147-148 (2009) 263-271.
[31] S. David, K. Sefiane, L. Tadrist, Experimental investigation of the effect of thermal properties of the substrate in the wetting and evaporation of sessile drops, Colloids and Surfaces A: Physicochemical and Engineering Aspects, 298 (2007) 108-114.
[32] E. Nefzaoui, O. Skurtys, Impact of a Liquid Drop on a Granular Medium: inertia, viscosity and surface tension effects on the drop deformation, ArXiv e-prints, (2010).
[33] D.C. Vadillo, A. Soucemarianadin, C. Delattre, D.C.D. Roux, Dynamic contact angle effects onto the maximum drop impact spreading on solid surfaces, Phys. Fluids, 21 (2009) 122002.
[34] A. Kukovecz, Z. Konya, N. Nagaraju, I. Willems, A. Tamasi, A. Fonseca, J.B. Nagy, I. Kiricsi, Catalytic synthesis of carbon nanotubes over Co, Fe and Ni containing conventional and sol-gel silica-aluminas, Phys. Chem. Chem. Phys., 2 (2000) 3071-3076.

[35] T. Kanyó, Z. Kónya, Á. Kukovecz, F. Berger, I. Dékány, I. Kiricsi, Quantitative Characterization of Hydrophilic−Hydrophobic Properties of MWNTs Surfaces, Langmuir, 20 (2004) 1656-1661.
[36] R. Smajda, Á. Kukovecz, Z. Kónya, I. Kiricsi, Structure and gas permeability of multi-wall carbon nanotube buckypapers, Carbon, 45 (2007) 1176-1184.
[37] A. Kukovecz, R. Smajda, M. Oze, B. Schaefer, H. Haspel, Z. Konya, I. Kiricsi, Multiwall carbon nanotube films surface-doped with electroceramics for sensor applications, Physica Status Solidi B-Basic Solid State Physics, 245 (2008) 2331-2334.
[38] R. Smajda, A. Kukovecz, B. Hopp, M. Mohl, Z. Konya, I. Kiricsi, Morphology and N-2 permeability of multi-wall carbon nanotube - Teflon membranes, Journal of Nanoscience and Nanotechnology, 7 (2007) 1604-1610.

Tables

Table 1. Physico-chemical properties of solvents used for evaporation profile measurement

	Molecular weight	Boiling point (°C)	Density ($g \cdot cm^{-3}$)	H_{vap} (kJ/mol)
1-propanol	60.095	97.20	0.7997	41.44
Acetone	58.079	56.05	0.7845	29.10
DMF	73.094	153.00	0.9445	46.89

Source: D.R. Lide, CRC Handbook of Chemistry and Physics, CRC Press, Boca Raton, 2005.

Table 2. Measured and calculated evaporation parameters for acetone, propanol and DMF

Solvent	m (mg)	V (μl)	Slope (Ω/mg)	h (μm)	r (mm)
Acetone	5	3	0.308 ± 0.070	80 ± 2	2.7 ± 0.1
1-propanol	3	3	0.462 ± 0.061	23 ± 3	3.3 ± 0.1
	5	3	0.303 ± 0.061	66 ±1	3.1 ± 0.3
	10	3	0.117 ± 0.025	180 ± 12	2.3 ± 0.1
	10	5	0.140 ± 0.015	136 ± 10	3.0 ± 0.1
DMF	5	3	0.385 ± 0.066	36 ± 1	4.9 ± 0.2
	10	3	0.267 ± 0.039	110 ± 11	3.1 ± 0.1
	10	5	0.542 ± 0.063	73 ± 4	3.9 ± 0.1

Figure captions

Fig. 1: Schematic view of the evaporation profile measurement setup.

Fig. 2: Images of the MWCNT film with a 1-propanol droplet spread on the surface (a), after the completion of primary surface evaporation (b) and after total evaporation from the pores (c). Field of view: 7.0 × 6.9 mm.

Fig. 3: Weight (a) and electrical resistance (b) variation of the buckypaper as functions of time. Experimental conditions: 3 μl 1-propanol droplet, 5 mg CNT film, 50 °C film temperature.

Fig. 4: Electrical resistance as a function of remaining solvent amount for a 5 mg CNT film and 50 °C film temperature.

Fig. 5: Difference between spot intensity and dry buckypaper image intensity as a function of spot radius (time series) (a), and the integrated spot intensity as a function of the remaining solvent weight (b).

Fig. 6: Reduction of the penetrative thickness of the liquid-filled area in buckypaper as a function of the droplet radius (time series).

Fig. 7: Characteristic weight variation as a function of time for three different solvents. Experimental conditions: 3 μl solvent drop, 5 mg CNT film, 50 °C film temperature.

Fig. 8: Electrical resistance as a function of remaining droplet weight in the case of acetone (a), 1-propanol (b), and DMF (c).

Fig. 9: The penetrative thickness of the liquid-filled area as a function of the wetted section radius for three different solvents.

Fig. 10: Sketch of the modeling mesh and the direction of current flow.

Fig. 11: Comparison of calculated and measured film resistance. Experimental conditions: 3 μl acetone droplet, 5 mg MWCNT buckypaper, 50 °C film temperature.

Fig. 12: The calculated dispersion of the specific conductivity viewed from above (a) and in cross-section (b) using data measured 16 s after placing a 3 µl 1-propanol droplet on a 5 mg CNT film.

Figure 1
Click here to download high resolution image

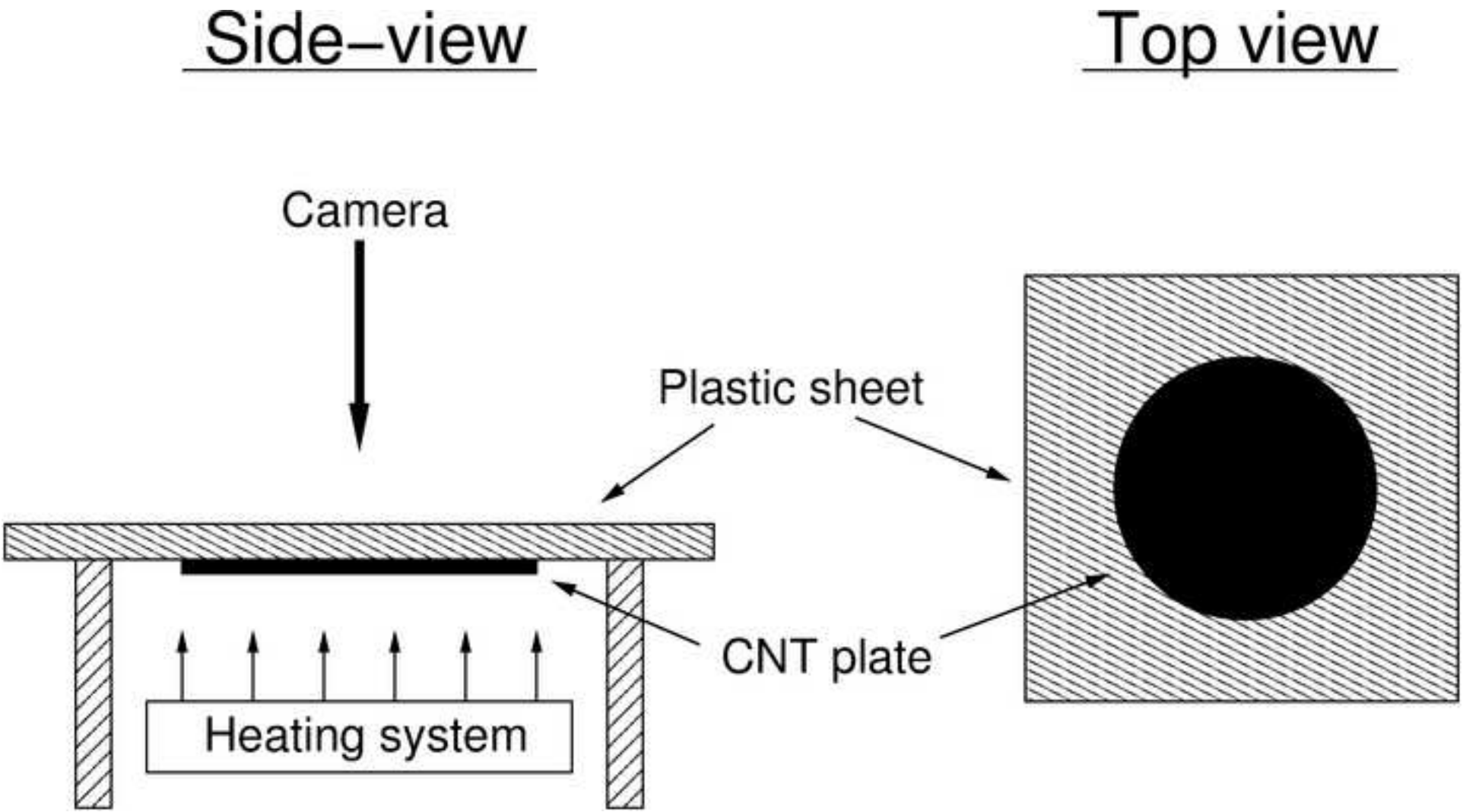

Figure 2
Click here to download high resolution image

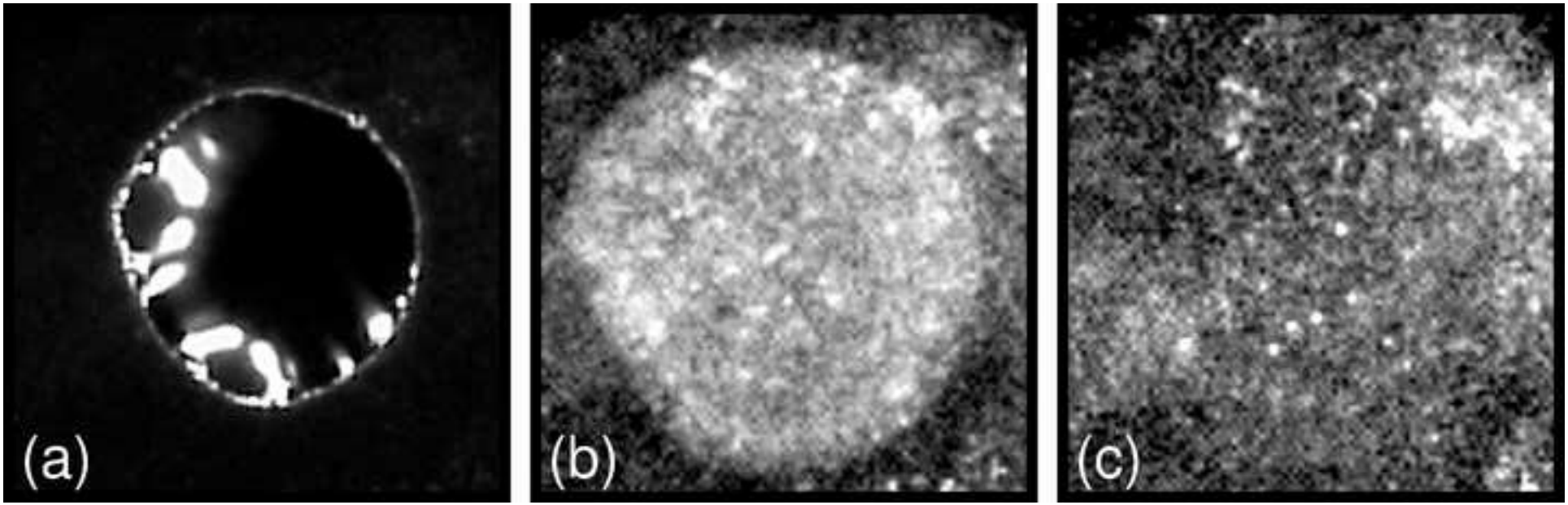

Figure 3
Click here to download high resolution image

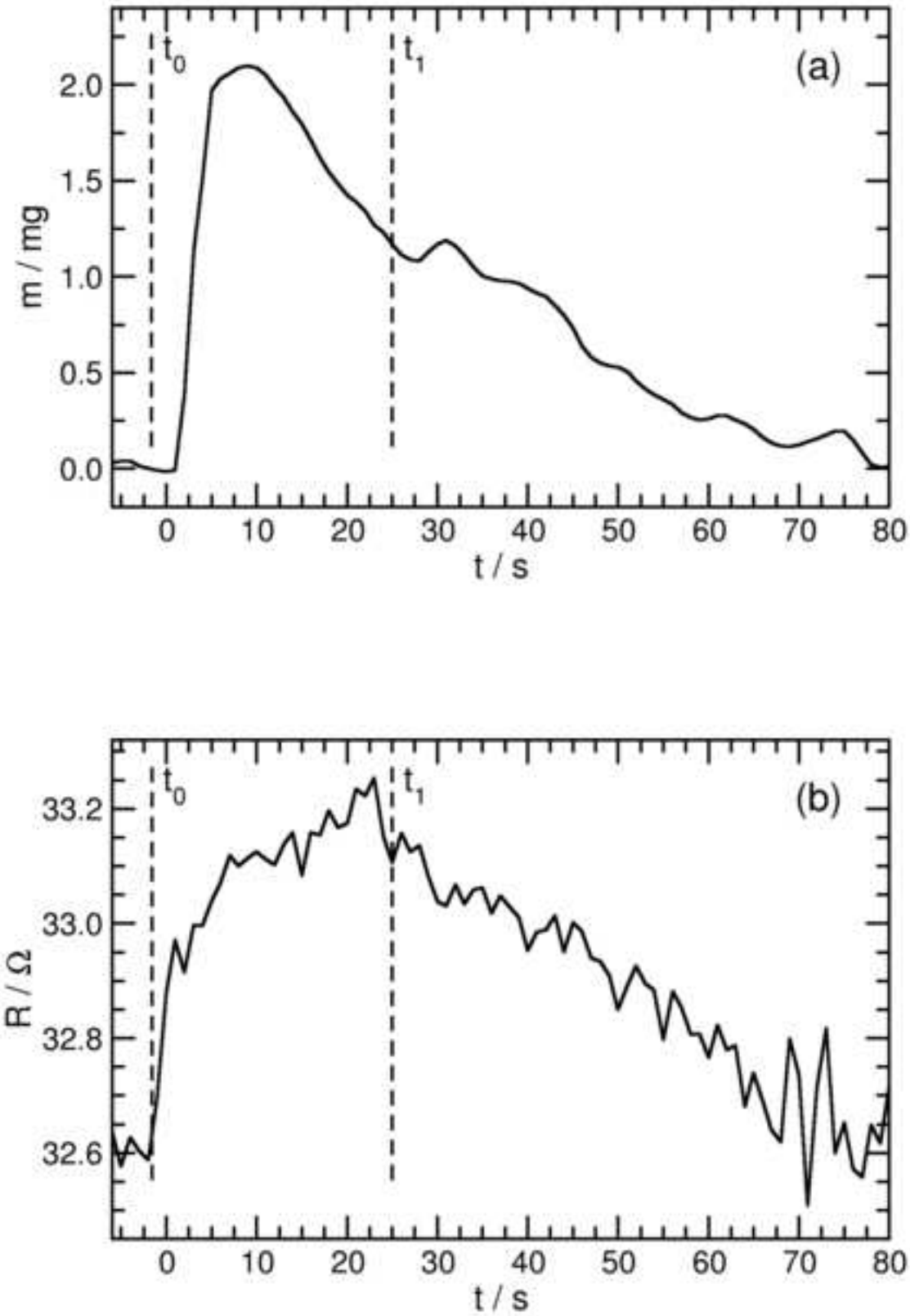

Figure 4
Click here to download high resolution image

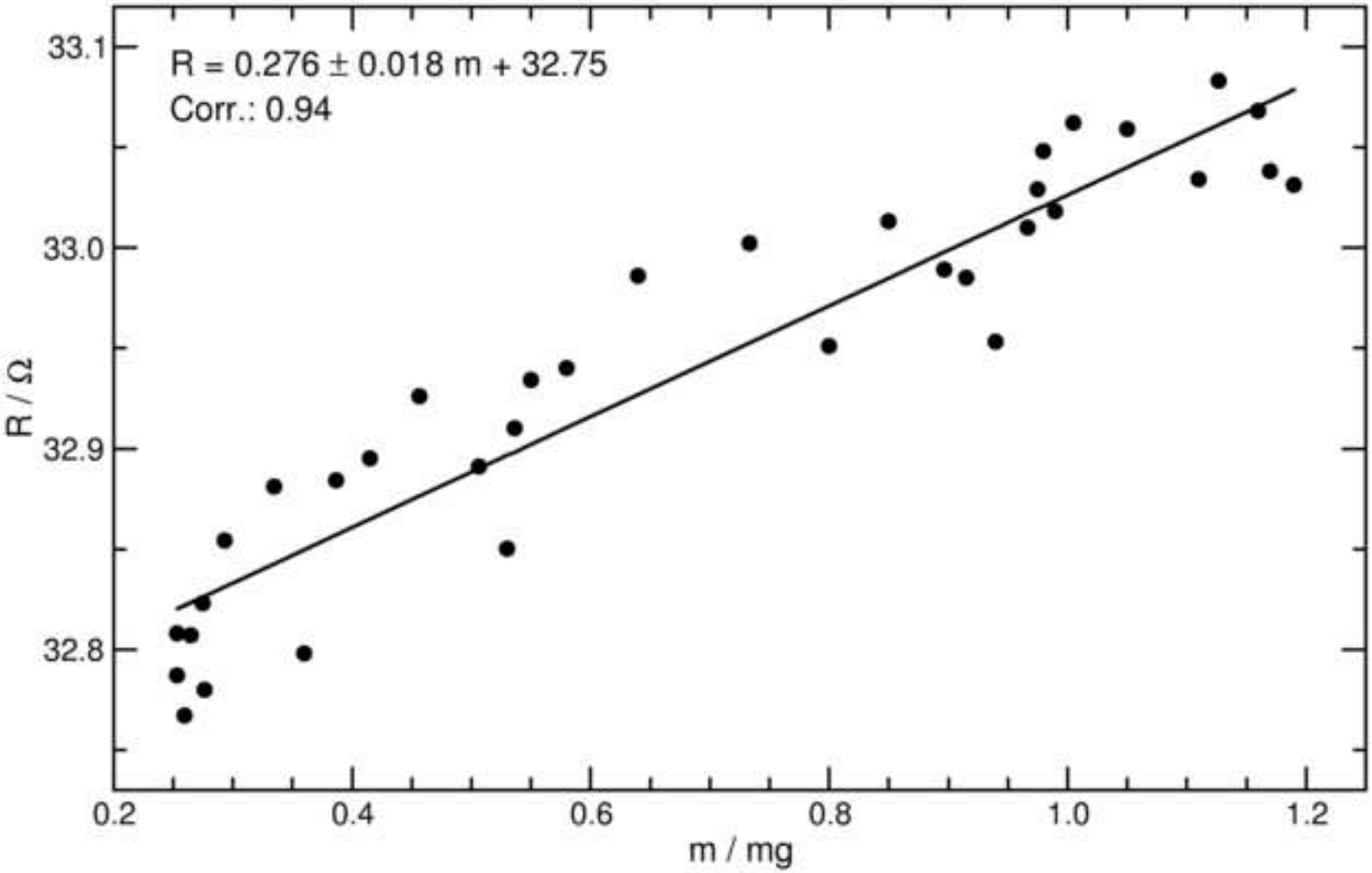

Figure 5
Click here to download high resolution image

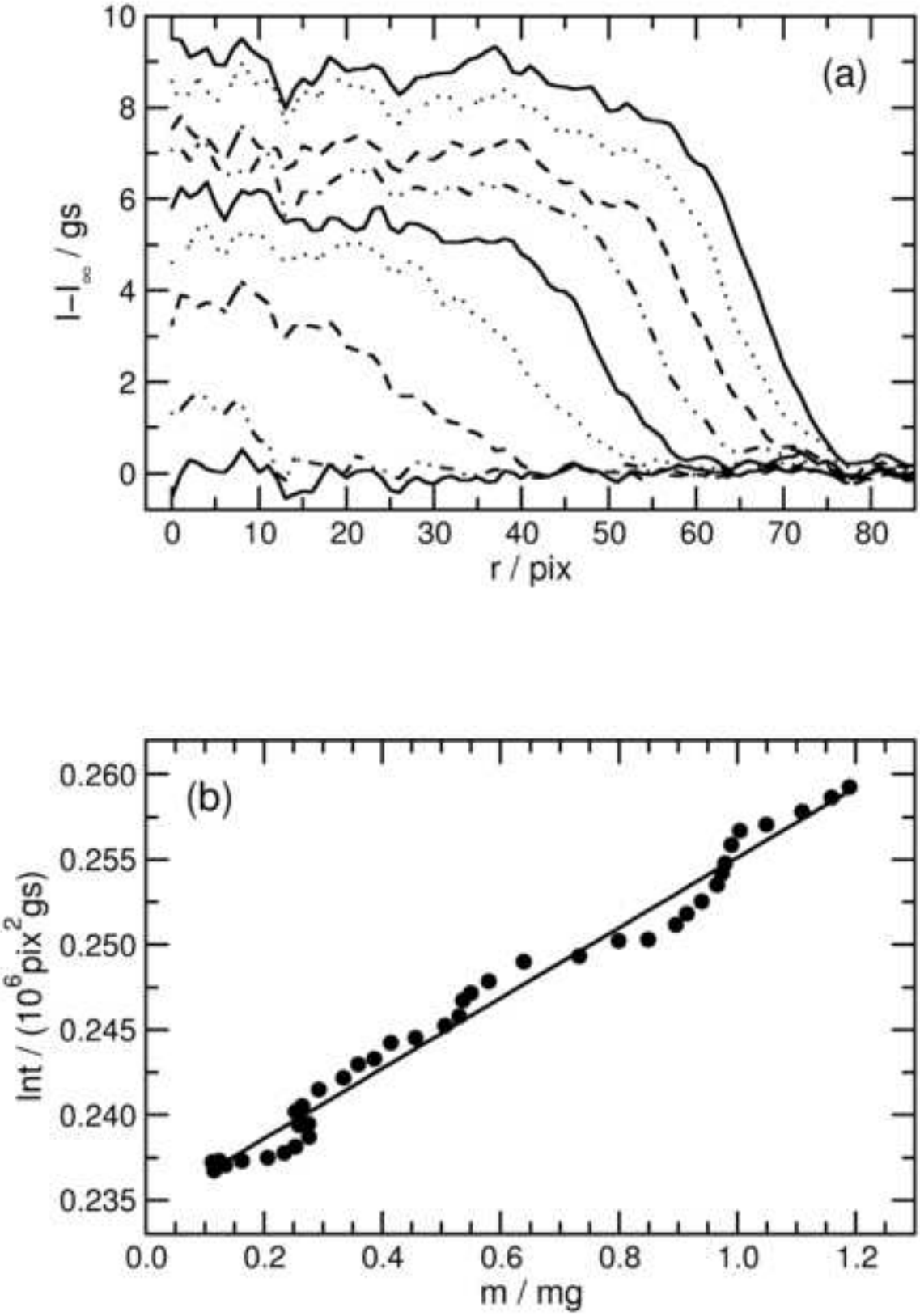

Figure 6
Click here to download high resolution image

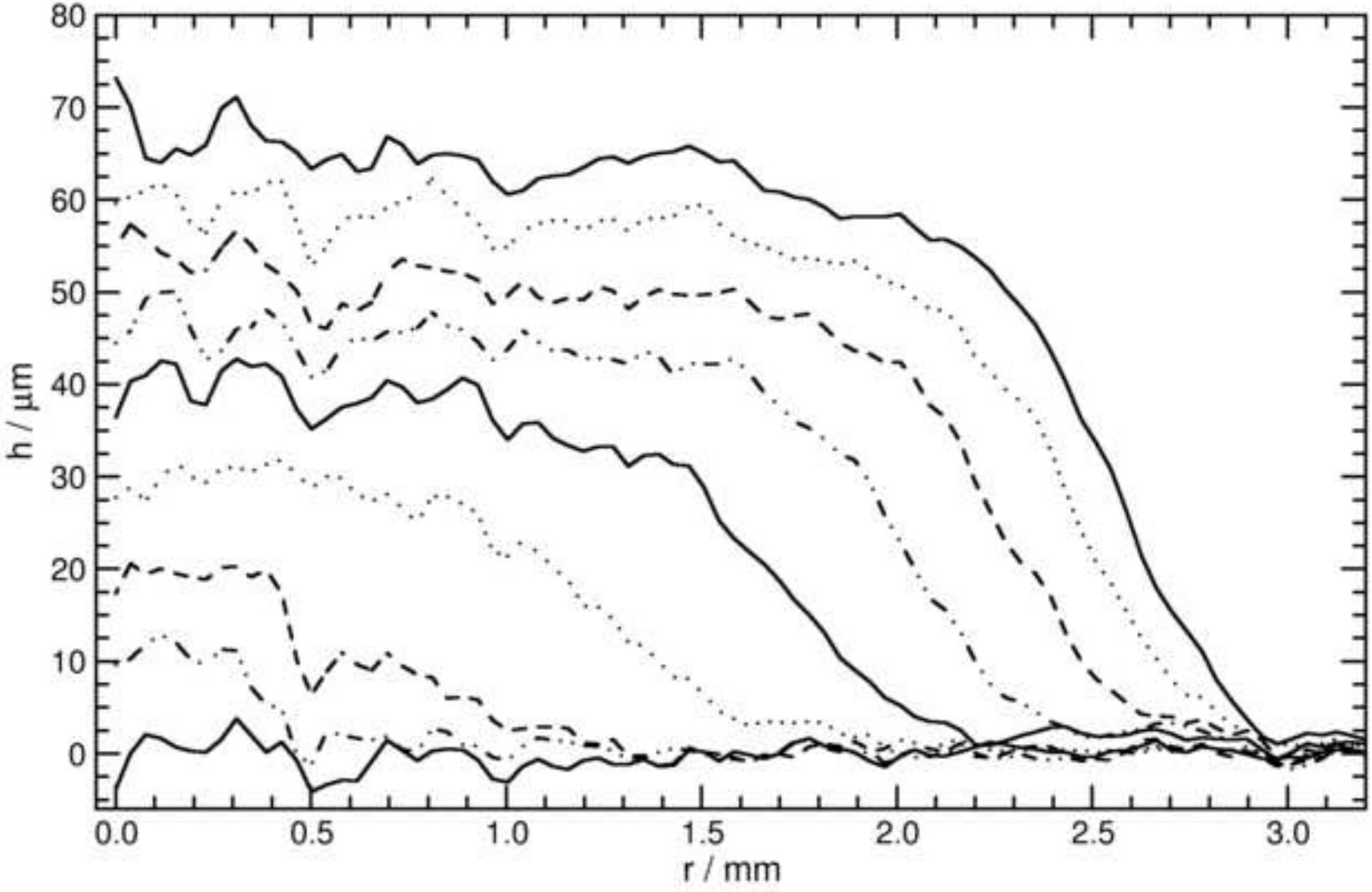

Figure 7
Click here to download high resolution image

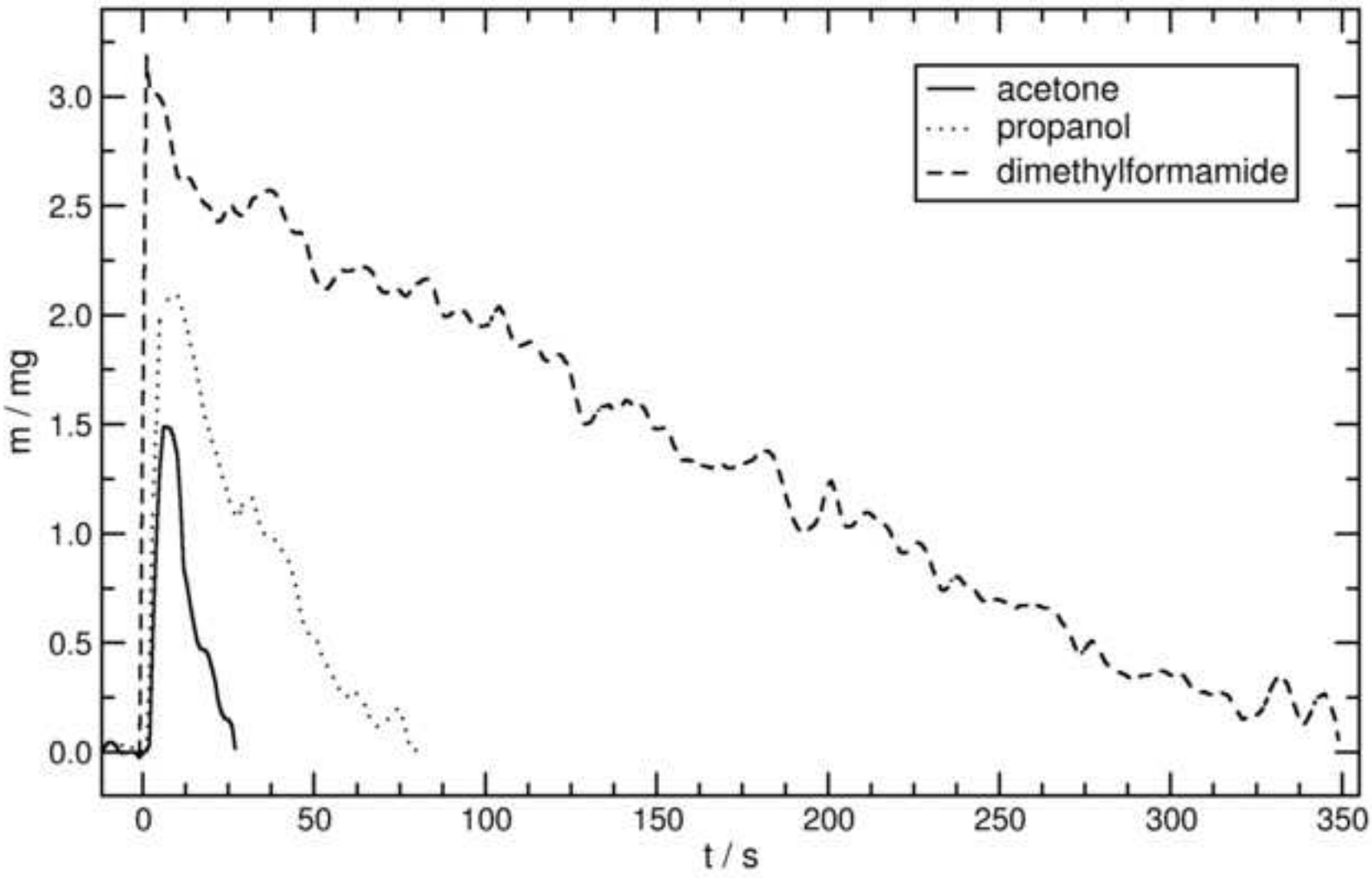

Figure 8
Click here to download high resolution image

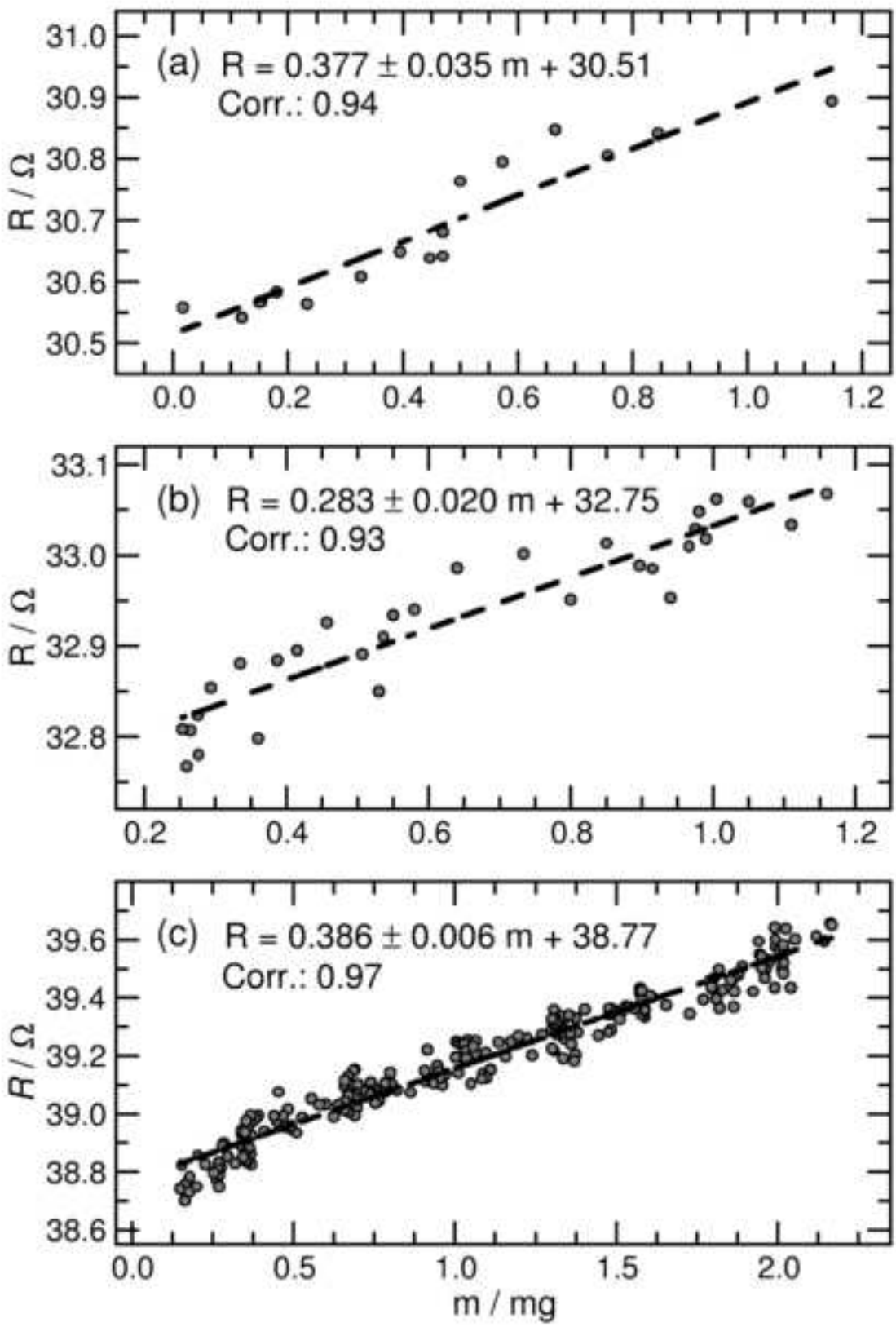

Figure 9
Click here to download high resolution image

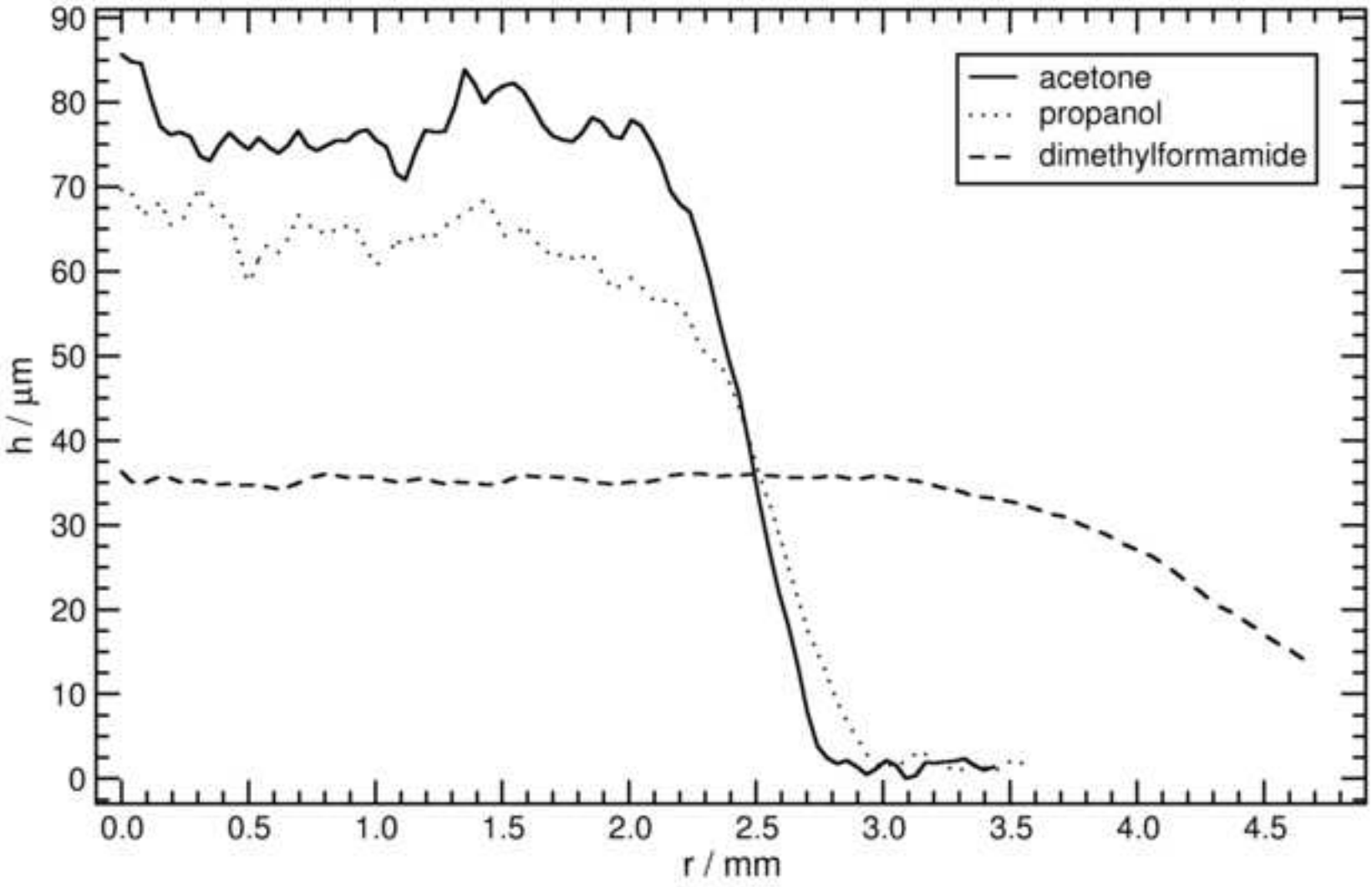

Figure 10
Click here to download high resolution image

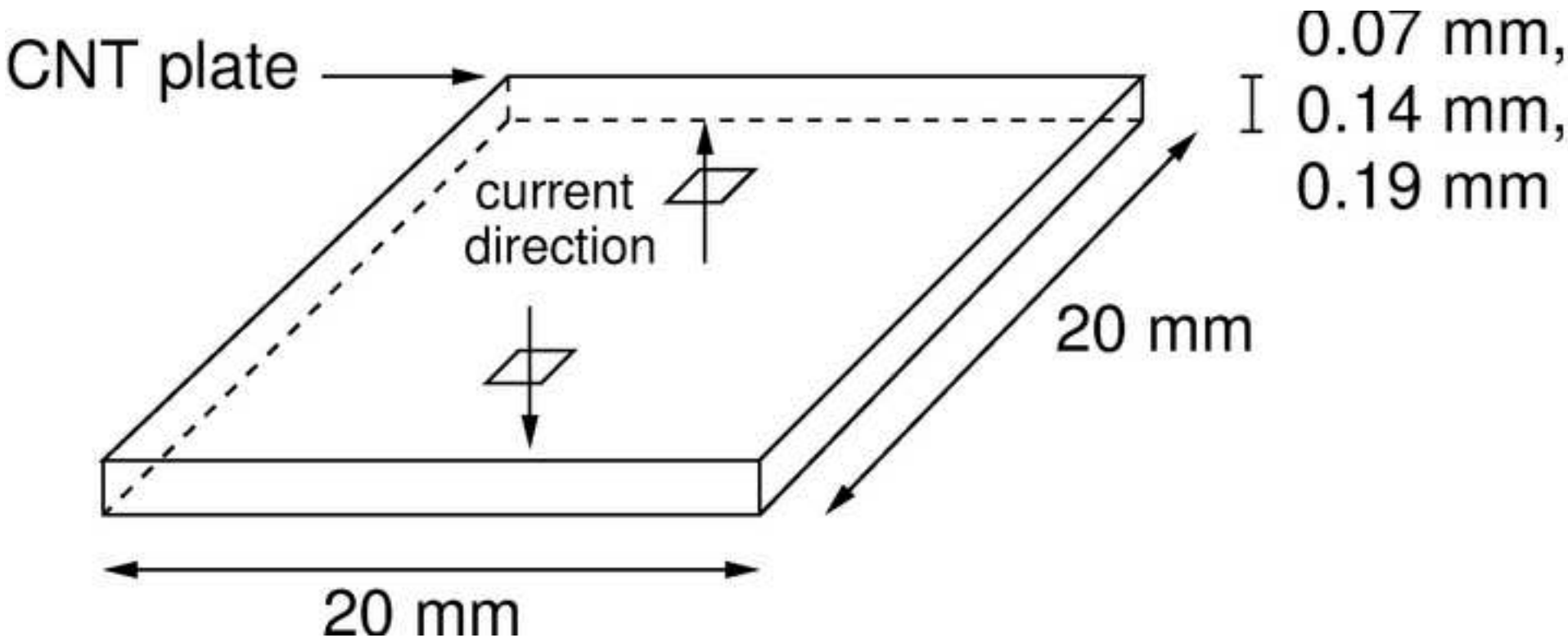

Figure 11
Click here to download high resolution image

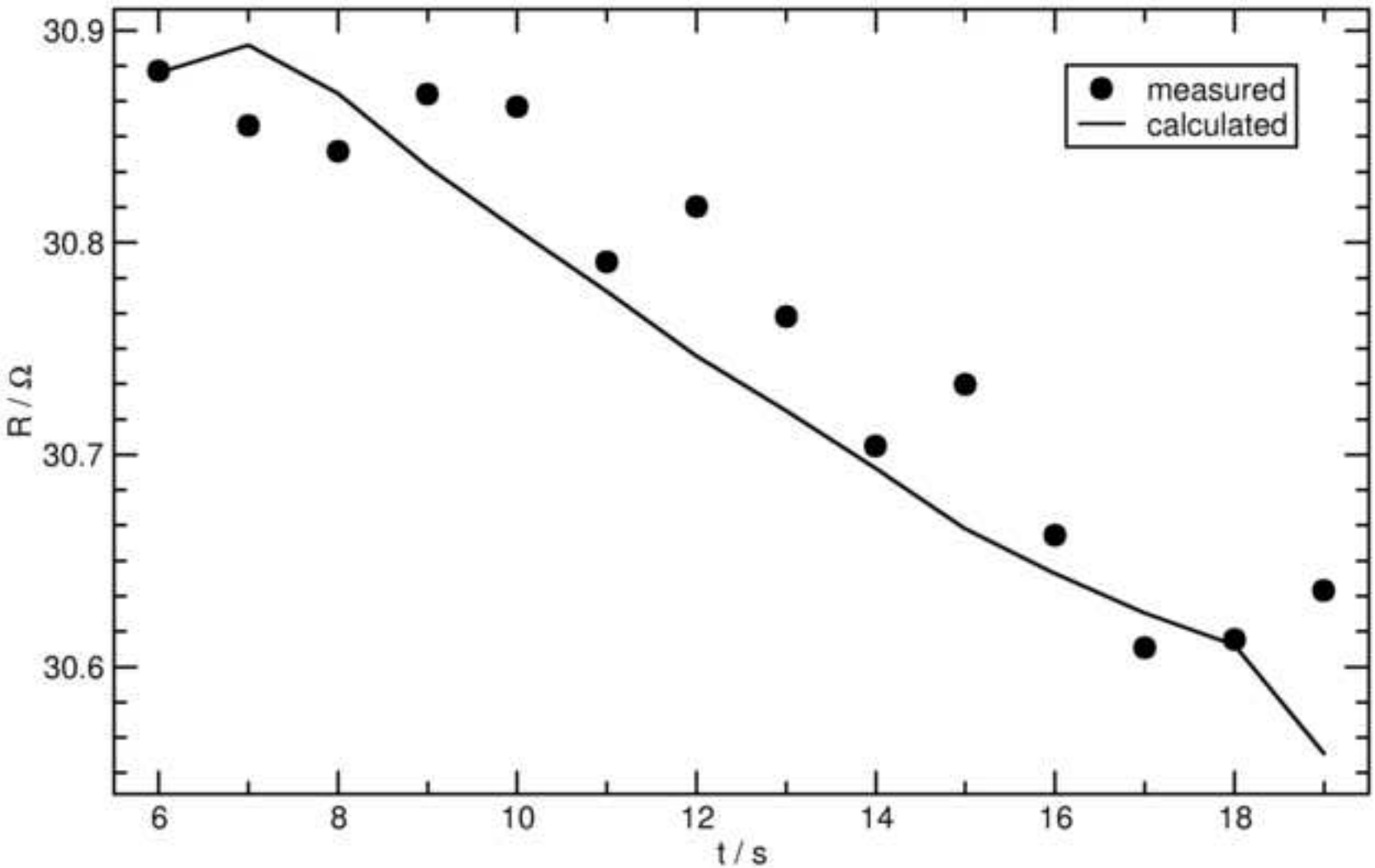

Figure 12
Click here to download high resolution image